Clinical and Experimental Obstetrics & Gynecology

Clin. Exp. Obstet. Gynecol. **2026**; 53(5): 47712
https://doi.org/10.31083/CEOG47712

Case Report

Identification of Novel Compound Heterozygous *ESCO2* Variants in a Chinese Family With Severe Prenatal Roberts–SC Phocomelia Syndrome and Successful Prevention Through Preimplantation Genetic Testing for Monogenic Disease

Ping Wang[1,2,†], Hong Liao[2,3,†], Xin Liu[1,2], Mei Yang[1,2], Xinlian Chen[1,2], He Wang[1,2], Hanbing Xie[1,2,*], Shanling Liu[1,2,*]

[1]Department of Medical Genetics/Prenatal Diagnostic Center, West China Second University Hospital, Sichuan University, 610041 Chengdu, Sichuan, China
[2]Key Laboratory of Birth Defects and Related Diseases of Women and Children (Sichuan University), Ministry of Education, 610041 Chengdu, Sichuan, China
[3]Department of Obstetrics and Gynecology, West China Second University Hospital, Sichuan University, 610041 Chengdu, Sichuan, China
*Correspondence: hb_tse@foxmail.com (Hanbing Xie); sunny630@126.com (Shanling Liu)
[†]These authors contributed equally.
Academic Editor: Michael H. Dahan
Submitted: 27 October 2025 Revised: 4 January 2026 Accepted: 16 January 2026 Published: 21 May 2026

Abstract

Background: Roberts–SC phocomelia syndrome (RBS; OMIM #268300) is a rare autosomal recessive disorder caused by biallelic variants in the sister chromatid cohesion N-acetyltransferase 2 (*ESCO2*) gene. It is characterized by tetraphocomelia and craniofacial anomalies. Prenatal cases are often lethal, and molecular confirmation is crucial for diagnosis and recurrence prevention. **Case**: We investigated a Chinese family with recurrent fetuses that presented severe tetraphocomelia. Whole-exome sequencing (WES) of both fetuses and their parents was performed, followed by Sanger validation, protein modeling using AlphaFold2, and Western blot analysis in transfected human embryonic kidney 293 (HEK293) cells. Two fetuses carried novel compound heterozygous nonsense variants in *ESCO2*, c.754A>T (p.Lys252*) and c.1276G>T (p.Glu426*). Structural modeling predicted truncated proteins lacking the C-terminal acetyltransferase domain. Western blot analysis showed that p.Lys252* caused complete loss of ESCO2, whereas p.Glu426* produced a truncated protein. Based on these findings, PGT-M was performed, identifying a mutation-free embryo for transfer. Prenatal testing confirmed the absence of *ESCO2* variants, and a healthy child was delivered. **Conclusions**: We report novel *ESCO2* variants associated with severe prenatal RBS and provide functional and clinical evidence supporting their pathogenicity. This study expands the *ESCO2* genotype–phenotype spectrum and underscores the value of molecular diagnosis and PGT-M in preventing recurrence of lethal autosomal recessive disorders.

Keywords: Roberts-SC phocomelia syndrome; whole-exome sequencing; *ESCO2*; preimplantation genetic testing; prenatal diagnosis

1. Introduction

Roberts syndrome is a rare autosomal recessive disorder first described by Roberts in 1919 [1]. Similar but milder phenotypes reported later are referred to as SC phocomelia. These conditions are now considered part of a continuous spectrum, collectively termed Roberts–SC phocomelia syndrome (RBS; OMIM #268300) [2]. Clinical features vary and may include tetraphocomelia (symmetrical limb reduction), pre- and postnatal growth retardation, craniofacial anomalies (microcephaly, cleft lip and palate), intellectual disability, congenital heart defects, and renal malformations [3]. Severe RBS often results in fetal or early neonatal death, whereas milder cases may survive to adulthood with varying degrees of intellectual disability [4]. The prenatal ultrasound features of severe RBS, such as tetraphocomelia and craniofacial abnormalities, can overlap with those of other conditions, including Cornelia de Lange syndrome and thrombocytopenia-absent radius syndrome. This overlap underscores the need for molecular diagnosis to enable accurate prenatal differentiation.

Biallelic variants in establishment of sister chromatid cohesion N-acetyltransferase 2 (*ESCO2*; OMIM #609353) cause RBS [5]. *ESCO2* comprises 11 exons and encodes an N-acetyltransferase of the Eco1/Ctf7 family. It contains a Cys2His2 (C2H2) zinc-finger–like motif and a conserved C-terminal acetyltransferase domain. This acetyltransferase activity is essential for the establishment of sister chromatid cohesion [6].

Herein, we describe three fetuses with severe tetraphocomelia from a Chinese family. Two fetuses carried novel compound heterozygous *ESCO2* variants (c.754A>T, p.Lys252*; c.1276G>T, p.Glu426*) identified by whole-exome sequencing (WES). Based on these findings, the family received preimplantation genetic testing for monogenic disease (PGT-M) and prenatal genetic diagnosis.

2. Materials and Methods

2.1 Whole-Exome Sequencing

Genomic DNA extracted from muscle tissue of the two fetuses and from peripheral blood from their parents was analyzed by WES. Fetal DNA samples underwent short tandem repeat (STR) analysis using quantitative fluorescent polymerase chain reaction (QF-PCR) to exclude maternal cell contamination. Exome enrichment was performed using the Nano WES Human Exome V2 kit (Berry Genomics, Guangzhou, Guangdong, China). Paired-end sequencing with 150-bp reads was performed on an Illumina NovaSeq 6000 platform (Illumina Inc., San Diego, CA, USA). Reads were aligned to the GRCh38/hg38 reference genome using the Burrows-Wheeler Aligner (BWA, Broad Institute, Cambridge, MA, USA). Variants were annotated using ANNOtate VARiation (ANNOVAR, University of Pennsylvania, Philadelphia, PA, USA) and the Enliven Variant Annotation and Interpretation System (Berry Genomics, Guangzhou, Guangdong, China). Population databases (gnomAD, 1000 Genomes) were used to filter rare variants. PubMed, ClinVar, OMIM, HGMD, and HGVS resources were consulted to evaluate variant pathogenicity. Variants were classified according to the American College of Medical Genetics and Genomics (ACMG) guidelines [7].

2.2 Structure Modeling With AlphaFold2

We predicted three-dimensional (3D) structures of wild-type (WT) and variant ESCO2 proteins using AlphaFold2 (https://colab.research.google.com/github/sokrypton/ColabFold/blob/main/AlphaFold2.ipynb). A TM-score >0.5 generally indicates similar folds, whereas lower TM-scores indicate structural divergence [8]. Root-mean-square deviation (RMSD) measures the structural difference between models; a smaller RMSD indicates closer structural similarity. Models were visualized with PyMOL(version 4.6, Schrödinger, New York, NY, USA).

2.3 Subcloning and Mutagenesis of ESCO2 cDNA

Human *ESCO2* cDNA (NM_001017420.3, 1806 bp) with an N-terminal His-tag was cloned into pcDNA3.1. Variants were generated using a high-fidelity PCR mix (#TSE101; Tsingke Biotechnology, Beijing, China). Primers were designed following standard site-directed mutagenesis principles. The target nucleotide substitution was positioned in the middle of the primer. Each side was flanked by 15–20 bp of perfectly matching sequence to ensure efficient and specific amplification. Primer design was performed using PrimerX to ensure optimal melting temperature, GC content, and minimal secondary structures. The c.754A>T variant was introduced with the following primers: F-5′-TGTAGAGACTGTCAGTGAATAAAAAACTTTTGCGA-3′ and R-5′-CTTGTCGCAAAAGTTTTTTATTCACTGA CGTCTC-3′. The c.1276G>T variant was introduced with the primers: F-5′-GTGGGTTGGAAGAAATAACGTGTAGTAGCAG-3′ and R-5′-CTGCTACTACACGTTATTTCTTCCAACCCA C-3′. PCR products were digested with DpnI to remove the template plasmid (#ER1702, Thermo Scientific, Waltham, MA, USA). Constructs corresponding to WT, c.754A>T, and c.1276G>T were verified by Sanger sequencing.

2.4 Cell Culture and Transfection

Human embryonic kidney 293 (HEK293) cells (GNHu-43; Chinese Academy of Sciences Cell Bank, Shanghai, China) were cultured in DMEM (#11,965,092, Gibco, Thermo Fisher Scientific, Waltham, MA, USA) supplemented with 10% fetal bovine serum (FBS) (#SFBS-NZ, Bovogen Biologicals Pty Ltd, Melbourne, Victoria, Australia), 100 U/mL penicillin, and 100 µg/mL streptomycin (#C0222, Beyotime Biotechnology, Shanghai, China), at 37 °C in 5% CO_2. Cells were transiently transfected in 6-well plates with 3 µg plasmid (WT or variant) or co-transfected with 1.5 µg of each variant plasmid using Lipofectamine 2000 (#11668019, Invitrogen, Thermo Fisher Scientific, Waltham, MA, USA) according to the manufacturer's instructions.

2.5 Western Blotting

At 24–36 hours post-transfection, cells were lysed in radio-immunoprecipitation assay (RIPA) buffer (#P0013B, Beyotime Biotechnology, Shanghai, China) supplemented with protease inhibitors (#P1005, Beyotime Biotechnology, Shanghai, China). 30 µg of protein lysate were separated by 8% sodium dodecyl sulfate–polyacrylamide gel electrophoresis (SDS-PAGE), transferred to nitrocellulose membranes, and blocked in 5% nonfat dry milk. Membranes were incubated with the following primary antibodies: anti-6X His-tag antibody (mouse monoclonal, 1:1000, #ab18184, Abcam, Cambridge, UK) and anti-β-actin (rabbit polyclonal, 1:1000, #4967, Cell Signaling Technology, Danvers, MA, USA). After washing, the membranes were incubated with the corresponding HRP-conjugated goat anti-mouse antibodies (1:1000, #A0216, Beyotime Biotechnology, Shanghai, China), and HRP-conjugated goat anti-rabbit antibodies (1:1000, #A0208, Beyotime Biotechnology, Shanghai, China). Bands were visualized using a ChemiDoc MP imaging system (Bio-Rad Laboratories Inc., Hercules, CA, USA).

2.6 Statistical Analysis

Western blotting was used for qualitative assessment of protein truncation and relative expression levels. Experiments were repeated in three independent replicates to ensure reproducibility.

2.7 PGT-M and Prenatal Genetic Diagnosis

Approximately 5–8 trophectoderm (TE) cells were biopsied from each blastocyst for whole-genome amplification (WGA) using multiple displacement amplification (REPLI-g Single Cell MDA kit, QIAGEN, Venlo, Lim-

burg, Netherlands). WGA products from parental oral mucosa and TE cells were analyzed by Sanger sequencing for validation of variant sites. Single nucleotide polymorphisms (SNP)-based haplotyping within a 1 Mb flanking region was performed using next-generation sequencing (NGS). NGS-based copy-number variants (CNVs) analysis screened for deletions and duplications >4 Mb. Amniocentesis in the second trimester was performed for fetal Sanger sequencing of the target variants, for chromosomal microarray analysis (CMA), and for karyotype analysis.

3. Case Presentation

3.1 Clinical Description

A 31-year-old woman (Fig. 1a,I-2) was referred for genetic counseling. In her first pregnancy, second-trimester ultrasound revealed tetraphocomelia, cleft lip and palate, and micrognathia, after which the pregnancy was terminated without prenatal diagnosis. A subsequent pregnancy in this couple was carefully monitored. At 12 weeks of gestation, ultrasound examination revealed dichorionic twins. One fetus presented nuchal translucency (NT) thickness of 3.3 mm, and the lengths of the upper and lower limbs were 5.7 mm and 3.8 mm, respectively. The other fetus also exhibited an increased NT (4.2 mm), with the upper and lower limbs lengths of 6.2 mm and 3.9 mm, respectively. Both fetuses lacked or had severely shortened humeri, ulnae, radii, femurs, tibiae, and fibulae. The pregnancy was terminated, and postmortem examination confirmed the ultrasound findings. No related clinical manifestations were observed in the parents or grandparents (pedigree shown in Fig. 1a).

3.2 Genetic Findings

WES was performed on muscle tissue from the twins and peripheral blood from their parents. WES identified two novel compound heterozygous *ESCO2* variants in the two probands: c.754A>T (p.Lys252*) and c.1276G>T (p.Glu426*). The father carried c.754A>T (p.Lys252*), and the mother carried c.1276G>T (p.Glu426*). Sanger sequencing validated the biallelic variants in the probands and confirmed parental carrier status (Fig. 1b). Both nonsense variants were classified as pathogenic according to ACMG criteria (PVS1 PM2_Supporting PP4).

3.3 Structure Predictions of ESCO2 Using AlphaFold2

AlphaFold2 predicted truncated ESCO2 structures for the p.Lys252* and p.Glu426* variants relative to the WT protein (Fig. 2). The highest-ranked p.Lys252* model aligned poorly with WT structure (TM-score 0.03; RMSD 0.66), and the p.Glu426* model also showed low similarity (TM-score 0.08; RMSD 16.63). The markedly reduced TM-scores indicate that both truncating variants lack the native global fold of ESCO2. RMSD values represent the extent of structural deviation within aligned regions and are influenced by alignment length. The elevated RMSD observed for the p.Glu426* variant reflects significant conformational alteration.

3.4 The c.1276G>T (p.Glu426) Variant in ESCO2 Gene Translates Into a Truncated Protein*

Western blotting analysis of HEK293 cell lysates showed a 72 kDa band corresponding to full-length ESCO2 in cells transfected with WT plasmid. A 50 kDa truncated band was detected in cells transfected with the p.Glu426* plasmid and in cells co-expressing both variants (p.Lys252* + p.Glu426*), albeit at low levels, suggesting partial escape from nonsense-mediated decay (NMD). No full-length or truncated ESCO2 was detected in cells expressing p.Lys252*, consistent with NMD-mediated loss of that transcript (Fig. 3). The p.Lys252*, located in exon 3, lies upstream of the acetyltransferase domain, whereas p.Glu426* (located in exon 8) truncates the protein within the acetyltransferase domain (Fig. 1c). Loss of ESCO2 acetyltransferase activity is likely central to RBS pathogenesis.

3.5 PGT-M and Prenatal Genetic Diagnosis

Based on the family's known *ESCO2* variants, PGT-M with concurrent CNV screening was performed. One blastocyst, graded 5BC, was free of both familial *ESCO2* variants and showed no clinically significant CNVs; this embryo was selected and transferred. Second-trimester prenatal diagnosis, including Sanger sequencing of targeted sites, CMA, and karyotype, confirmed the absence of the familial *ESCO2* variants and chromosomal abnormalities. Prenatal ultrasound findings remained unremarkable. At the last follow-up, the child was three years old and showed no features observed in the affected probands (Fig. 1a,II-4).

4. Discussion

We identified compound heterozygous *ESCO2* variants (c.754A>T, p.Lys252*; c.1276G>T, p.Glu426*) in two fetuses with RBS. Both variants introduce premature termination codons: c.754A>T (p.Lys252*) likely causes mRNA instability through NMD, whereas c.1276G>T (p.Glu426*) yields a truncated protein that lacks part of the acetyltransferase domain.

RBS exhibits wide clinical variability. *ESCO2* encodes an N-acetyltransferase that contains a zinc-finger–like motif and a C-terminal acetyltransferase domain. In this study, structural predictions yielded extremely low TM-scores for both truncating variants. This finding indicates a complete loss of the native ESCO2 structural framework and suggests severe disruption of the functional acetyltransferase domain [9]. Western blot analysis supported these predictions and revealed distinct molecular consequences for the two nonsense variants. The p.Lys252* variant resulted in undetectable ESCO2 protein, which is consistent with NMD, whereas the p.Glu426* variant produced a truncated protein, suggesting partial escape

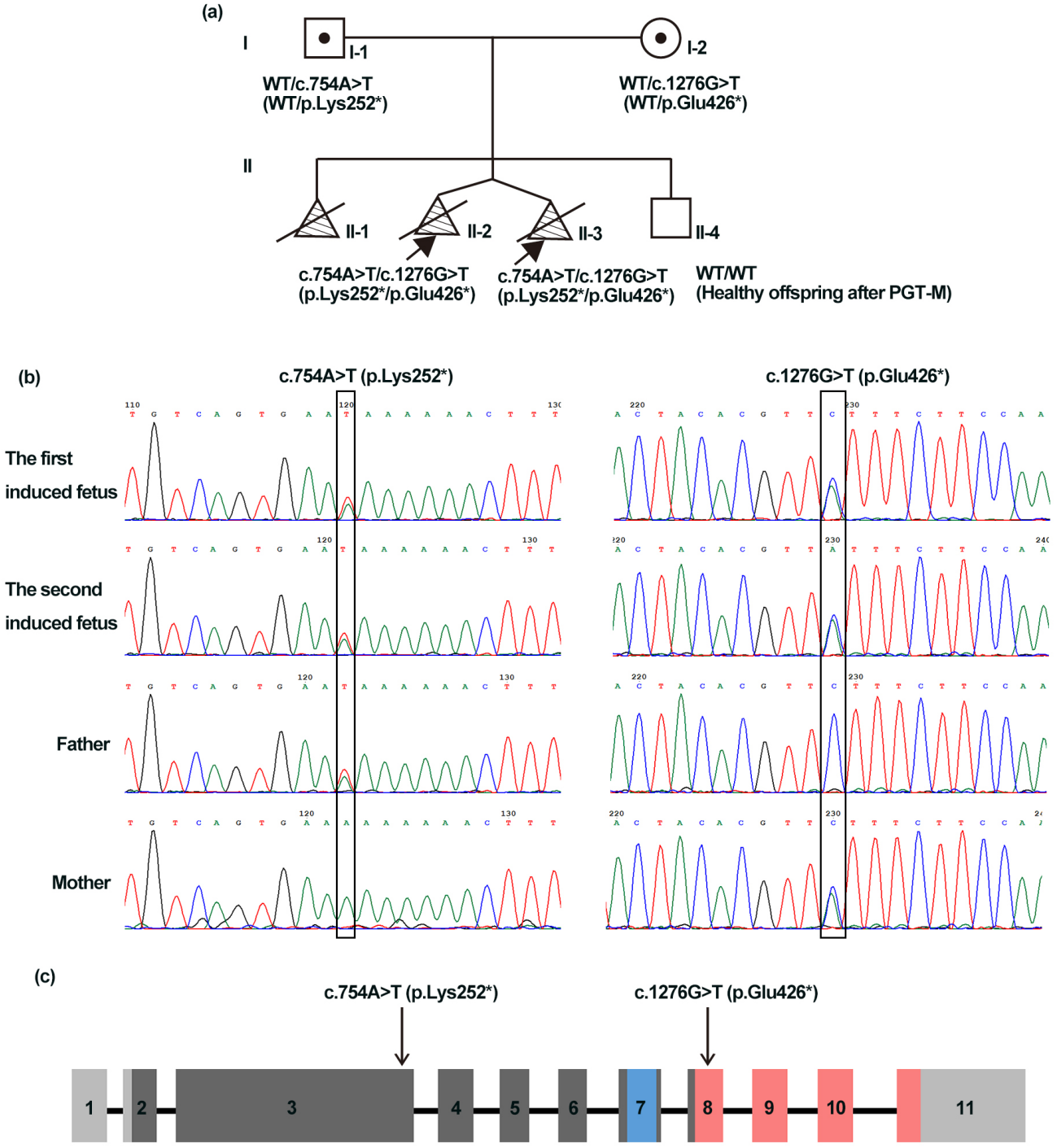

Fig. 1. Clinical characteristics of the family and schematic of the establishment of sister chromatid cohesion N-acetyltransferase 2 (*ESCO2*). (a) Pedigree that shows compound heterozygous *ESCO2* variants (c.754A>T, p.Lys252* and c.1276G>T, p.Glu426*); probands are indicated by arrows. The unaffected offspring (II-4) was born following preimplantation genetic testing for monogenic disease (PGT-M). (b) Sanger sequencing traces of *ESCO2* in family members confirm biallelic variants in probands and heterozygous carrier status in parents. (c) Schematic of *ESCO2* structure: UTRs (light grey), coding regions (dark grey) and introns (lines). Functional domains are indicated: C2H2 zinc-finger-like (blue) and acetyltransferase domain (pink); variant positions are marked. PGT-M, preimplantation genetic testing for monogenic disease; WT, wild-type; UTRs, untranslated regions. In the pedigree, Roman numerals (I, II) indicate different generations. Arabic numerals (e.g., 1, 2, 3, 4) indicate individuals within each generation. Therefore, I-1 and I-2 represent individuals 1 and 2 in the first generation, and II-1, II-2, II-3, and II-4 represent individuals 1, 2, 3, and 4 in the second generation, respectively.

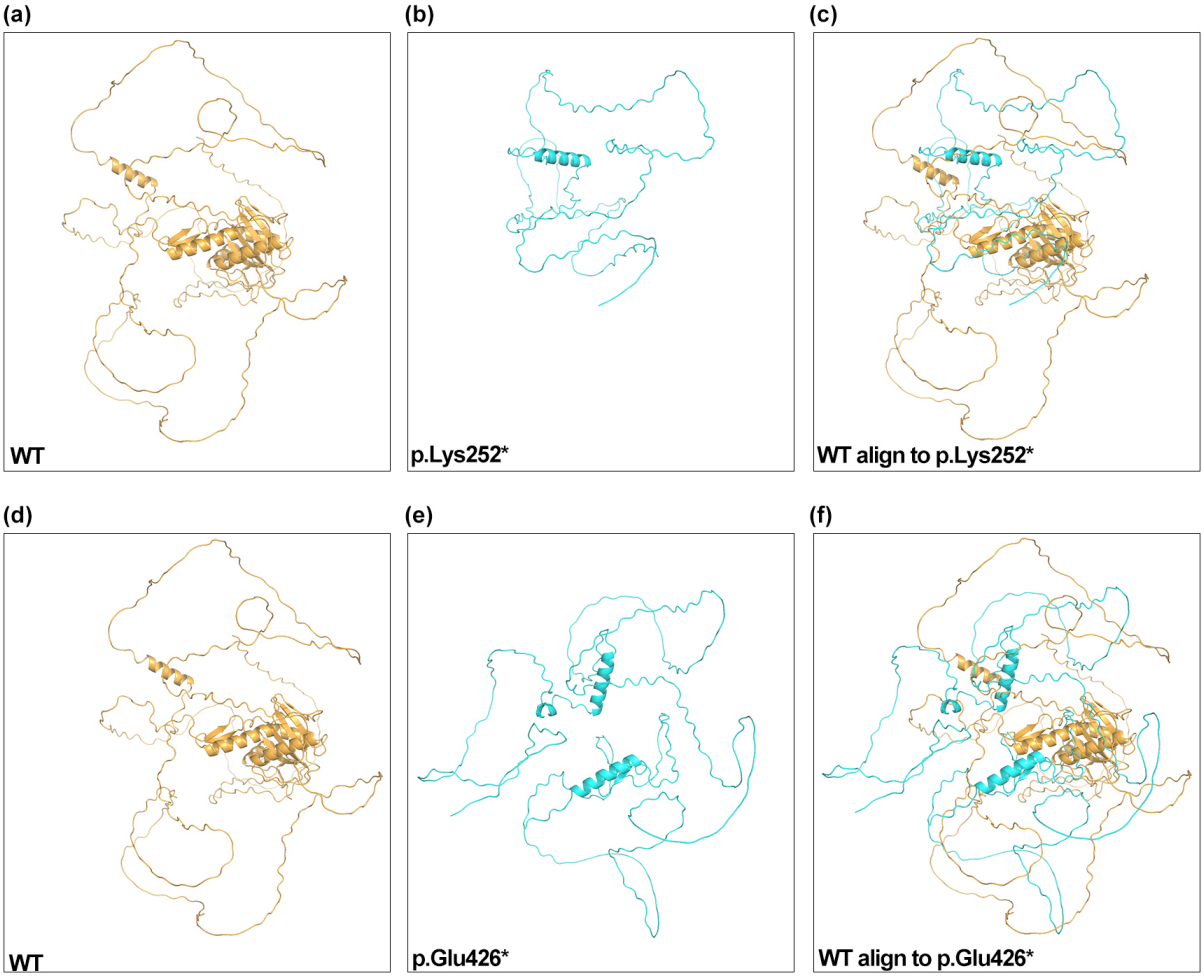

Fig. 2. AlphaFold2 structural models of ESCO2. Predicted structures for WT (a,d), p.Lys252* (b), p.Glu426* (e), and structural alignments (c,f) are shown. Two views of the WT structure are displayed for clarity. WT, wild-type.

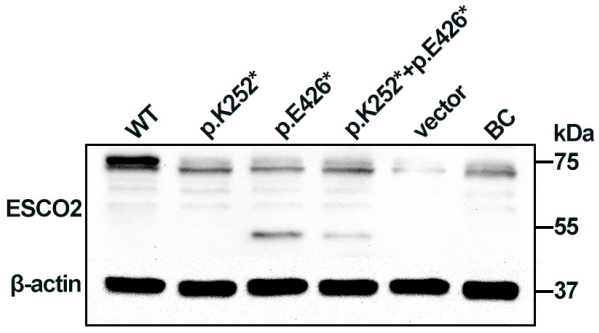

Fig. 3. Western blot analysis of ESCO2 expression in human embryonic kidney 293 (HEK293) cells. Cell extracts were probed with an anti-6X His tag antibody. A 72 kDa band corresponding to full-length ESCO2 was observed in cells transfected with the WT plasmid. A 50 kDa truncated band was detected in cells transfected with p.Glu426* and with the combined (p.Lys252* + p.Glu426*) constructs. β-actin served as a loading control. WT, wild-type; vector, empty vector; BC, blank control.

from NMD. Despite these differences in protein expression, both variants are expected to severely compromise acetyltransferase function. This provides a plausible molecular mechanism for the RBS phenotype observed in this family.

To explore genotype–phenotype correlations, we reviewed *ESCO2* variants reported in HGMD and the literature (accessed October 2025; Table 1, Ref. [4,10–33]). Approximately 43 likely pathogenic or pathogenic *ESCO2* variants have been reported to date. The variant spectrum comprises small deletions/insertions that cause frameshifts (25/43; 58.14%), splicing variants (7/43; 16.28%), nonsense variants (5/43; 11.63%), missense variants (5/43; 11.63%), and in-frame deletions (1/43; 2.33%). Most pathogenic variants are null alleles that truncate the protein or cause mRNA instability, and many occur upstream of or within the acetyltransferase domain [10]. However, genotype or variant location alone does not reliably predict clinical severity, as both severe prenatal phenotypes and milder postnatal presentations have been observed across similar classes of variants. Consistent with previous reports, no clear genotype–phenotype correlation has been established for *ESCO2* variants [11,12].

Table 1. *ESCO2* variants identified in individuals with RBS.

ID	Variants	Exon	Tetraphocomelia	Growth retardation	Craniofacial abnormalities	Cleft palate/lip	Mental retardation	Others
1	c.505C>T(p.Arg169*)	ex 3	NA	NA	NA	NA	NA	[13]
2	c.604C>T(p.Gln202*)	ex 3	+	+	+	–	±	hemangioma [14]
3	c.1166G>A(p.Cys389Tyr)	ex 7	NA	NA	NA	NA	NA	[15]
4	c.1220A>T(p.His407Leu)	ex 7	+	+	+	–	+	cerebrovascular diseases [16]
5	c.1269G>A(p.Trp423*)	ex 8	NA	NA	NA	NA	NA	[17]
6	c.1489A>T(p.Ile497Phe)	ex 9	NA	NA	NA	NA	NA	[18]
7	c.1567C>T(p.Gln523*)	ex 10	NA	NA	NA	NA	NA	[19]
8	c.1615T>G(p.Trp539Gly)	ex 10	NA	NA	NA	NA	NA	[10,20,21]
9	c.1654C>T(p.Arg552*)	ex 10	+	+	–	+	+	seizure [22]
10	c.1741G>C(p.Gly581Arg)	ex 11	+	NA	NA	NA	NA	[11]
11	c.1131+1G>A	int 6	+	+	+	NA	±	prominent eyes [12]
12	c.1132-7A>G	int 6	+	+	+	–	NA	[12]
13	c.1263+1G>C	int 7	NA	NA	NA	NA	NA	[17]
14	c.1354-18G>A	int 8	NA	NA	NA	NA	NA	[10]
15	c.1673+1G>A	int 10	+	+	–	–	–	[23]
16	c.1674-2A>G	int 10	NA	NA	NA	NA	NA	[10]
17	c.166_170del(p.Val56fs)	ex 3	–	+	–	–	±	cardiac abnormalities [4]
18	c.252_253del(p.Ser85fs)	ex 3	+	NA	NA	NA	NA	[20]
19	c.294_297del(p.Arg99fs)	ex 3	NA	NA	NA	NA	NA	[10]
20	c.307_311del(p.Lys103fs)	ex 3	NA	NA	NA	NA	NA	[13]
21	c.308_309del(p.Lys103fs)	ex 3	NA	NA	NA	NA	NA	[10]
22	c.417del(p.Lys139fs)	ex 3	+	+	+	–	+	[24]
23	c.745_746del(p.Val249fs)	ex 3	+	+	–	–	NA	[25]
24	c.752del(p.Lys253fs)	ex 3	+	+	+	–	±	hemangioma [14]
25	c.760del(p.Thr254fs)	ex 3	NA	NA	NA	NA	NA	[13]
26	c.764_765del(p.Phe255fs)	ex 3	+	+	+	+	+	[26]
27	c.876_879del(p.Asp292fs)	ex 4	+	+	+	+	–	[27]
28	c.879_880del(p.Arg293fs)	ex 4	+	+	–	+	–	[20]
29	c.955+2_955+5del	int 4	NA	NA	NA	NA	NA	[13]

Table 1. Continued.

ID	Variants	Exon	Tetraphocomelia	Growth retardation	Craniofacial abnormalities	Cleft palate/lip	Mental retardation	Others
30	c.1156del(p.Ala386fs)	ex 7	NA	NA	NA	NA	NA	[28]
31	c.1359_1361del(p.Glu453del))	ex 7	NA	NA	NA	NA	NA	[11]
32	c.1461_1462del(p.Arg487fs)	ex 9	+	NA	NA	NA	NA	[20]
33	c.1562del(p.Ala521fs)	ex 10	+	+	+	–	+	cerebrovascular diseases [16]
34	c.244_245dup(p.Thr83fs)	ex 3	+	+	+	+	+	blue sclera [26]
35	c.417dup(p.Pro140fs)	ex 3	NA	NA	NA	NA	NA	[29]
36	c.416_417dup(p.Pro140fs)	ex 3	NA	NA	NA	NA	NA	[29]
37	c.636dup(p.Val213fs)	ex 3	NA	NA	NA	NA	NA	[20]
38	c.751dup(p.Glu251fs)	ex 3	NA	NA	NA	NA	NA	[30]
39	c.760dup(p.Thr254fs)	ex 3	+	+	+	+	–	cardiac anomalies [26,31]
40	c.877dup(p.Arg293fs)	ex 4	NA	NA	NA	NA	NA	[32]
41	c.1111_1112insG(p.Thr371fs)	ex 6	NA	NA	NA	NA	NA	[10]
42	c.1111dup(p.Thr371fs)	ex 6	+	+	+	+	NA	[33]
43	c.1597dup(p.Cys533fs)	ex 10	NA	NA	NA	NA	NA	[10]

Abbreviation: Ex, exon; Int, intron; +, feature is present; –, feature is absent; ±, mild phenotype; NA, no available information; RBS, Roberts–SC phocomelia syndrome.

Data sources: Variants were collated from the HGMD professional database and the published literature (up to October 2025).

Nevertheless, when variant distribution and functional domains are considered together, a consistent pathogenic mechanism emerges. Regardless of variant type (e.g., frameshift, nonsense, splicing, or missense), most pathogenic *ESCO2* variants are expected to impair or abolish acetyltransferase activity, either through NMD, protein truncation, or direct disruption of the catalytic domain. This convergence on loss of acetyltransferase function suggests that impaired ESCO2-mediated acetylation represents the core pathogenic mechanism underlying RBS, even in the absence of a strong genotype–phenotype correlation. The phenotypic variability may therefore reflect differences in residual activity and modifying genetic or environmental factors, rather than variant class or position alone.

Prenatal diagnosis of RBS is challenging because tetraphocomelia and growth restriction overlap with several other syndromes (e.g., Cornelia de Lange syndrome, CHARGE syndrome, thrombocytopenia-absent radius syndrome). Therefore, genetic testing is essential for accurate prenatal diagnosis [34]. In this family, recurrent severe tetraphocomelia prompted WES, which identified causative *ESCO2* variants and enabled PGT-M and prenatal diagnosis. These measures successfully prevented recurrence and resulted in the birth of a healthy infant.

Limitations

A limitation of this study is the lack of additional functional assays that assess ESCO2 acetyltransferase activity. Such experiments would provide more direct mechanistic evidence linking the observed nonsense variants to loss of enzymatic function and RBS pathogenesis.

5. Conclusions

In summary, we describe novel compound heterozygous *ESCO2* variants associated with severe prenatal RBS and demonstrate the value of molecular diagnosis to guide reproductive decision-making and prevent recurrence.

Availability of Data and Materials

The data and materials that support the findings of this study are available from the corresponding authors upon reasonable request.

Author Contributions

Conceptualization: SL, HX, HW, XC, MY, PW, HL, XL; Methodology: PW, XL; Writing-original draft preparation: PW, HL; Writing-review and editing: SL, HX, HW; Funding acquisition: SL; Supervision: SL, HX. All authors contributed to critical revision of the manuscript for important intellectual content. All authors read and approved the final manuscript. All authors have participated sufficiently in the work and agreed to be accountable for all aspects of the work.

Ethics Approval and Consent to Participate

The study was carried out in accordance with the guidelines of the Declaration of Helsinki. The study was approved by the ethical committee of West China Second University Hospital, Sichuan University (Medical Research Ethics Review 2024 No. 228). In addition, the family signed written informed consent to participate.

Acknowledgment

Not applicable.

Funding

This study was supported by the National Key Research and Development Program of China (2022YFC2703302).

Conflicts of Interest

The authors declare no conflicts of interest.

Declaration of AI and AI-Assisted Technologies in the Writing Process

During the preparation of this work, the authors used ChatGPT-3.5 in order to check spelling and grammar. After using this tool, the authors reviewed and edited the content as needed and take full responsibility for the content of the publication.

Supplementary Material

Supplementary material associated with this article can be found, in the online version, at https://doi.org/10.31083/CEOG47712.

References

[1] Allingham-Hawkins DJ, Tomkins DJ. Somatic cell hybridization of Roberts syndrome and normal lymphoblasts resulting in correction of both the cytogenetic and mutagen hypersensitivity cellular phenotypes. Somatic Cell and Molecular Genetics. 1991; 17: 455–462. https://doi.org/10.1007/BF01233169.

[2] Van Den Berg DJ, Francke U. Roberts syndrome: a review of 100 cases and a new rating system for severity. American Journal of Medical Genetics. 1993; 47: 1104–1123. https://doi.org/10.1002/ajmg.1320470735.

[3] McDaniel LD, Prueitt R, Probst LC, Wilson KS, Tomkins D, Wilson GN, *et al*. Novel assay for Roberts syndrome assigns variable phenotypes to one complementation group. American Journal of Medical Genetics. 2000; 93: 223–229. https://doi.org/10.1002/1096-8628(20000731)93:3<223::aid-ajmg13>3.0.co;2-j.

[4] Goh ESY, Li C, Horsburgh S, Kasai Y, Kolomietz E, Morel CF. The Roberts syndrome/SC phocomelia spectrum–a case report of an adult with review of the literature. American Journal of Medical Genetics. Part a. 2010; 152A: 472–478. https://doi.org/10.1002/ajmg.a.33261.

[5] Strasser AS, Gonzalez-Reiche AS, Zhou X, Valdebenito-Maturana B, Ye X, Zhang B, *et al*. Limb reduction in an Esco2 cohesinopathy mouse model is mediated by p53-dependent apoptosis and vascular disruption. Nature Communications. 2024; 15: 7154. https://doi.org/10.1038/s41467-024-51328-3.

[6] Hou F, Zou H. Two human orthologues of Eco1/Ctf7 acetyltransferases are both required for proper sister-chromatid cohesion. Molecular Biology of the Cell. 2005; 16: 3908–3918. https://doi.org/10.1091/mbc.e04-12-1063.

[7] Richards S, Aziz N, Bale S, Bick D, Das S, Gastier-Foster J, *et al*. Standards and guidelines for the interpretation of sequence variants: a joint consensus recommendation of the American College of Medical Genetics and Genomics and the Association for Molecular Pathology. Genetics in Medicine. 2015; 17: 405–424. https://doi.org/10.1038/gim.2015.30.

[8] Xu J, Zhang Y. How significant is a protein structure similarity with TM-score = 0.5? Bioinformatics (Oxford, England). 2010; 26: 889–895. https://doi.org/10.1093/bioinformatics/btq066.

[9] Zhang Y, Skolnick J. Scoring function for automated assessment of protein structure template quality. Proteins. 2004; 57: 702–710. https://doi.org/10.1002/prot.20264.

[10] Gordillo M, Vega H, Trainer AH, Hou F, Sakai N, Luque R, *et al*. The molecular mechanism underlying Roberts syndrome involves loss of ESCO2 acetyltransferase activity. Human Molecular Genetics. 2008; 17: 2172–2180. https://doi.org/10.1093/hmg/ddn116.

[11] Vega H, Trainer AH, Gordillo M, Crosier M, Kayserili H, Skovby F, *et al*. Phenotypic variability in 49 cases of ESCO2 mutations, including novel missense and codon deletion in the acetyltransferase domain, correlates with ESCO2 expression and establishes the clinical criteria for Roberts syndrome. Journal of Medical Genetics. 2010; 47: 30–37. https://doi.org/10.1136/jmg.2009.068395.

[12] Schüle B, Oviedo A, Johnston K, Pai S, Francke U. Inactivating mutations in ESCO2 cause SC phocomelia and Roberts syndrome: no phenotype-genotype correlation. American Journal of Human Genetics. 2005; 77: 1117–1128. https://doi.org/10.1086/498695.

[13] Capalbo A, Valero RA, Jimenez-Almazan J, Pardo PM, Fabiani M, Jiménez D, *et al*. Optimizing clinical exome design and parallel gene-testing for recessive genetic conditions in preconception carrier screening: Translational research genomic data from 14,125 exomes. PLoS Genetics. 2019; 15: e1008409. https://doi.org/10.1371/journal.pgen.1008409.

[14] Parry DM, Mulvihill JJ, Tsai SE, Kaiser-Kupfer MI, Cowan JM. SC phocomelia syndrome, premature centromere separation, and congenital cranial nerve paralysis in two sisters, one with malignant melanoma. American Journal of Medical Genetics. 1986; 24: 653–672. https://doi.org/10.1002/ajmg.1320240410.

[15] Saini N, Venkatapuram VS, Vineeth VS, Kulkarni A, Tandon A, Koppolu G, *et al*. Fetal phenotypes of Mendelian disorders: A descriptive study from India. Prenatal Diagnosis. 2022; 42: 911–926. https://doi.org/10.1002/pd.6172.

[16] He S, Chen S, Li SJ, Zhang JW, Liang XL. Complex cerebrovascular diseases in Roberts syndrome caused by novel biallelic ESCO2 variations. Molecular Genetics & Genomic Medicine. 2023; 11: e2177. https://doi.org/10.1002/mgg3.2177.

[17] Xiong HY, Alipanahi B, Lee LJ, Bretschneider H, Merico D, Yuen RKC, *et al*. RNA splicing. The human splicing code reveals new insights into the genetic determinants of disease. Science (New York, N.Y.). 2015; 347: 1254806. https://doi.org/10.1126/science.1254806.

[18] Molina-Ramírez LP, Kyle C, Ellingford JM, Wright R, Taylor A, Bhaskar SS, *et al*. Personalised virtual gene panels reduce interpretation workload and maintain diagnostic rates of proband-only clinical exome sequencing for rare disorders. Journal of Medical Genetics. 2022; 59: 393–398. https://doi.org/10.1136/jmedgenet-2020-107303.

[19] Stranneheim H, Lagerstedt-Robinson K, Magnusson M, Kvarnung M, Nilsson D, Lesko N, *et al*. Integration of whole genome sequencing into a healthcare setting: high diagnostic rates across multiple clinical entities in 3219 rare disease patients. Genome Medicine. 2021; 13: 40. https://doi.org/10.1186/s13073-021-00855-5.

[20] Vega H, Waisfisz Q, Gordillo M, Sakai N, Yanagihara I, Yamada M, *et al*. Roberts syndrome is caused by mutations in ESCO2, a human homolog of yeast ECO1 that is essential for the establishment of sister chromatid cohesion. Nature Genetics. 2005; 37: 468–470. https://doi.org/10.1038/ng1548.

[21] van der Lelij P, Godthelp BC, van Zon W, van Gosliga D, Oostra AB, Steltenpool J, *et al*. The cellular phenotype of Roberts syndrome fibroblasts as revealed by ectopic expression of ESCO2. PloS One. 2009; 4: e6936. https://doi.org/10.1371/journal.pone.0006936.

[22] Kantaputra PN, Dejkhamron P, Tongsima S, Ngamphiw C, Intachai W, Ngiwsara L, *et al*. Juberg-Hayward syndrome and Roberts syndrome are allelic, caused by mutations in ESCO2. Archives of Oral Biology. 2020; 119: 104918. https://doi.org/10.1016/j.archoralbio.2020.104918.

[23] Schneeberger PE, Nayak SS, Fuchs S, Kutsche K, Girisha KM. Roberts syndrome in an Indian patient with humeroradial synostosis, congenital elbow contractures and a novel homozygous splice variant in ESCO2. American Journal of Medical Genetics. Part a. 2020; 182: 2793–2796. https://doi.org/10.1002/ajmg.a.61826.

[24] Colombo EA, Mutlu-Albayrak H, Shafeghati Y, Balasar M, Piard J, Gentilini D, *et al*. Phenotypic Overlap of Roberts and Baller-Gerold Syndromes in Two Patients With Craniosynostosis, Limb Reductions, and *ESCO2* Mutations. Frontiers in Pediatrics. 2019; 7: 210. https://doi.org/10.3389/fped.2019.00210.

[25] Resta N, Susca FC, Di Giacomo MC, Stella A, Bukvic N, Bagnulo R, *et al*. A homozygous frameshift mutation in the ESCO2 gene: evidence of intertissue and interindividual variation in Nmd efficiency. Journal of Cellular Physiology. 2006; 209: 67–73. https://doi.org/10.1002/jcp.20708.

[26] Afifi HH, Abdel-Salam GMH, Eid MM, Tosson AMS, Shousha WG, Abdel Azeem AA, *et al*. Expanding the mutation and clinical spectrum of Roberts syndrome. Congenital Anomalies. 2016; 56: 154–162. https://doi.org/10.1111/cga.12151.

[27] da Costa Almeida CB, Welter AT, Abech GD, Brandão GR, Flores JAM, Schüle B, *et al*. Report of the Phenotype of a Patient with Roberts Syndrome and a Rare *ESCO2* Variant. Journal of Pediatric Genetics. 2020; 9: 58–62. https://doi.org/10.1055/s-0039-1696636.

[28] Scocchia A, Kangas-Kontio T, Irving M, Hero M, Saarinen I, Pelttari L, *et al*. Diagnostic utility of next-generation sequencing-based panel testing in 543 patients with suspected skeletal dysplasia. Orphanet Journal of Rare Diseases. 2021; 16: 412. https://doi.org/10.1186/s13023-021-02025-7.

[29] Kalayci T, Altunoglu U, Çorbacioglu Esmer A, Avcı Ş, Sarac Sivrikoz T, Karaman B, *et al*. Fetal skeletal dysplasia cohort of a single tertiary referral center in Istanbul, Turkey. American Journal of Medical Genetics. Part a. 2023; 191: 498–509. https://doi.org/10.1002/ajmg.a.63050.

[30] Kars ME, Başak AN, Onat OE, Bilguvar K, Choi J, Itan Y, *et al*. The genetic structure of the Turkish population reveals high levels of variation and admixture. Proceedings of the National Academy of Sciences of the United States of America. 2021; 118: e2026076118. https://doi.org/10.1073/pnas.2026076118.

[31] McKay MJ, Craig J, Kalitsis P, Kozlov S, Verschoor S, Chen P, *et al*. A Roberts Syndrome Individual With Differential Genotoxin Sensitivity and a DNA Damage Response Defect. International Journal of Radiation Oncology, Biology, Physics. 2019; 103: 1194–1202. https://doi.org/10.1016/j.ijrobp.2018.11.047.

[32] Mengen E, Kotan LD, Ucakturk SA, Topaloglu AK, Yuksel B. A Novel Frameshift Mutation in ESCO2 Gene in Roberts Syndrome. Journal of the College of Physicians and Surgeons–Pakistan: JCPSP. 2018; 28: 403–405. https://doi.org/10.29271/

jcpsp.2018.05.403.
[33] Zhu L, Cao D, Chen M, Zhang H, Sun X, Liu W. Prenatal diagnosis of Roberts syndrome in a Chinese family based on ultrasound findings and whole exome sequencing: a case report. BMC Medical Genomics. 2022; 15: 16. https://doi.org/10.1186/s12920-022-01161-8.
[34] Wu XJ, Li JR, Tan J, Tang P. Next-Generation Sequencing to Determine the Genetic Etiology of Fetal Skeletal Abnormalities Detected by Prenatal Ultrasound. Clinical and Experimental Obstetrics & Gynecology. 2025; 52: 39131. https://doi.org/10.31083/CEOG39131.